Improvement of sintering, nonlinear electrical, and dielectric properties of ZnO-based varistors doped with TiO_2

Osama A Desouky[1,†] and K E Rady[2]

[1] *Bilbis Higher Institute of Engineering (BHIE), Bilbis, Sharqia, Egypt*
[2] *Engineering Basic Sciences Department, Faculty of Engineering, Menoufia University, Shebin El-Kom, Egypt*

(Received 22 October 2015; revised manuscript received 27 January 2016; published online 20 April 2016)

The effects of TiO_2 on sintering and nonlinear electrical properties of $(98.5-x)$ZnO–0.5MnO_2–0.5Co_2O_3-0.5Bi_2O_3–$x$$TiO_2$ ($x = 0.3, 0.5, 0.7, 0.9$ mol%) ceramic varistors prepared by the ceramic technique are investigated in this work. The optimum sintering temperature of the prepared samples is deduced by determining the firing shrinkage and water absorption percentages. The optimum sintering temperature is found to be 1200 °C, at which each of the samples shows a maximum firing shrinkage and minimum water absorption. Also minimum water absorption appears in a sample of $x = 0.9$ mol%. Higher sintering temperature and longer sintering time give rise to a reduction in bulk density due to the increased amount of porosity between the large grains of ZnO resulting from the rapid grain growth induced by the liquid phase sintering. The crystal size of ZnO decreases with increasing TiO_2 doping. The addition of TiO_2 improves the nonlinear coefficient and attains its maximum value at $x = 0.7$ mol% of TiO_2, further addition negatively affects it. A decrease in capacitance consequently in the dielectric constant is recorded with increasing the frequency in a range of 30 kHz–200 kHz. The temperature and composition dependences of the dielectric constant and AC conductivity are also studied. The increase of temperature raises the dielectric constant because it increases ionic response to the field at any particular frequency.

Keywords: ZnO varistors, water absorption, nonlinear electrical properties, dielectric constant

PACS: 84.32.Ef, 78.20.Ci, 77.55.hf **DOI:** 10.1088/1674-1056/25/6/068402

1. Introduction

Zinc oxide (ZnO) ceramics with certain additives exhibit strong non-Ohmic conductions and, therefore, these materials are used for fabricating varistors-transient voltage suppression devices.[1–3] ZnO-based varistor ceramics are obtained by adding a small quantity of oxides of Bi, Sb, Ti, Co, Mn, Ni, Cr, Al, and others into ZnO powder, and then sinters it in air at the temperature ranging from 1100 °C to 1300 °C, typically at 1200 °C. The current-voltage nonlinearity of the varistor is a grain-boundary phenomenon with an ideal breakdown voltage of the grain boundary being about 3.2 V.[4–8] The majority of commercial ZnO varistors necessarily contain Bi_2O_3 as varistor-forming oxides and they exhibit excellent varistor properties. However, they have a few drawbacks due to the high volatility and reactivity of Bi_2O_3 melted at about 825 °C during a sintering above 1000 °C.[9] The former changes the varistor characteristics with the variation of the inter-composition ratio of additives, the latter destroys the multi-layer structure of chip varistors and it generates many secondary phases in addition to insulating the spinel phase deteriorating surge-absorption capabilities. The Bi_2O_3 is an essential additive of the ZnO varistor. Because Bi_2O_3 has a melting point that is far lower than those of ZnO and other additives, it exists in liquid phase in a relatively low temperature, which promotes other oxides to be distributed evenly in the ZnO grains and grain boundary.[10,11] The nonlinear current–voltage (I–V) behavior of ZnO varistors is derived from the addition of a small quantity of other metal oxides,[12] such as Bi_2O_3, Sb_2O_3, and Co_3O_4 since a dopant is responsible for the formation of varistor behavior.[13] It is believed that for the application of the ZnO varistors, the dopant plays an important role in modifying the defect concentration at the ZnO grain and/or of grain boundary where the performance of ZnO is sensitive to the presence of some additives even when their quantities are very low.[14] Pure ZnO is a nonstoichiometric n-type semiconductor with a linear V–I behavior. To make it nonlinear, various additive oxides are incorporated into the ZnO. Moreover, the incorporation of these oxides causes atomic defects to form in the grain and at the grain boundary, with donor or donor-like defects dominating in the depletion layer and acceptor and acceptor-like defects dominating at the grain - boundary. From a study of the defect equilibria in ZnO, Einzinger[15] has demonstrated that a defect-induced potential barrier can be formed from the unequal migration of defects toward the grain boundary. TiO_2 is commonly used as a grain growth enhancing additive in ZnOBi_2O_3-based varistor ceramic.[16,17] This effect is attributed to the increased reactivity of the Bi_2O_3-rich liquid phase by introducing the titanium ions that are rapidly distributed into the liquid phase and increase the chemical activity of ZnO particles and thus accelerate their growth.[18–20] The microstructure and electrical properties of zinc oxide varistor ceramic can be modified by adding various metal oxides. As is well known the co-addition of praseodymium and cobalt into pure zinc oxide essentially induces nonlinear properties from Ohmic properties, in the voltage–current relation.[6–10] The adding of various rare earth oxides can noticeably increase the breakdown field, and

†Corresponding author. E-mail: Osama_Amin2015@yahoo.com

© 2016 Chinese Physical Society and IOP Publishing Ltd

improve the nonlinear coefficient.[21–30] The sintering temperature has a prominent effect on the electrical properties of ZnO varistor. According to the SEM and XRD analysis, if the temperature is too high, many of the Bi atoms will volatilize, and thus bring about many air pores in the ZnO varistor to deteriorate the structural uniformity, thereby affecting its electrical properties.[31,32]

The aim of the present work is to investigate the effects of TiO_2 doping on the sintering temperature nonlinear electrical and dielectric properties of ZnO–MnO_2–Co_2O_3–Bi_2O_3-based ceramic varistors.

2. Material and methods

The powders were obtained by the conventional oxide mixing method through using the following compounds ZnO(Sigma-Aldrich)–MnO_2–Co_2O_3 (vetec), Bi_2O_3(Sigma-Aldrich), and TiO_2 (Merck). The samples were prepared using a conventional ceramic technique with a nominal composition of $(98.5-x)$ZnO–0.5MnO_2–0.5Co_2O_3–0.5Bi_2O_3 – $x$$TiO_2$ ($x = 0.3, 0.5, 0.7, 0.9$ mol% of TiO_2) and named A_1, A_2, A_3, and A_4 respectively. The raw material powders of analytical grade were mixed and ball-milled in water for 4 h with high-resistant ZrO_2 balls as the medium. The resulting slurries were dried in air at 200 °C for at least 24 h, and then calcined in air at 750 °C for 2 h. The calcined mixtures were crashed into powders, sieved, and pressed into discs of 1.2 cm in diameter and 0.3 cm in thickness. These discs were processed by a semi-dry press method under 70KN. Then, the discs were sintered at 900 °C–1200 °C for 2 h. The optimum sintering temperature for all the samples was deduced from the determination of the following parameters: firing shrinkage and water absorption percentages. The method given is based on the ASTM standard (C71, C72). The structures of the prepared samples were identified using XRD on a Brucker axis D8 diffractometer of Cu-K_α radiation ($\lambda = 1.5418$ Å). Mean grain size was determined by analyzing the SEM micrographs (Joel-JEM. T200). To perform the electrical measurements, silver contacts were deposited on the sample surfaces. The I–V measurements of these samples were made by using a DC power supply in a current range up to 2 mA. The non-linearity index α) was calculated from the following equation:

$$\alpha = (\log I_2 - \log I_1)/(\log V_2 - \log V_1),$$

where V_1 and V_2 are the potential differences corresponding to the electric currents I_1 and I_2 respectively in the on-state (high voltage) region.

A PM 6304 programmable automatic RCL meter was used for accurately measuring the resistance, capacitance and inductance. From the measured values of the capacitance, the dielectric constants at all frequencies ranging from 30 kHz to 200 kHz were calculated at a constant temperature. The relative permittivity (ε') and conductivity σ were calculated from the following relations: $\varepsilon' = Cd/\varepsilon_0 A$, where C is the capacitance in unit F, d is the thickness of specimen in unit m, $\varepsilon_0 = 8.85 \times 10^{-12}$ F/m, and A is the area of specimen in unit m^2. Also from the values of resistance R, conductivity σ was calculated from the following relation: $\sigma = d/RA$.

3. Results and discussion

Results of physical properties indicate that better densification takes place in discs fired at 1200 °C for 2 h above which they start to deform. Low water absorption values are achieved for all mixes. Therefore, this temperature is selected as the proper maturing temperature for them. Water absorptions of different mixes decrease with increasing firing temperature and mol% of TiO_2, i.e., addition of TiO_2 in present Co_2O_3, MnO_2, and Bi_2O_3 leads to better densification by minimizing the presence of closed pores. Minimum water absorption appears in sample (A_4) of $x = 0.9$ mol% which equals 1.02, fired at 1200 °C for 2 h. It is evident that better densifications and minimum water absorptions are achieved in all mixes fired at 1200 °C for 2 h as shown in Fig. 1(a). Also results of firing shrinkage as a function of temperature show that the shrinkage increases with temperature increasing. Maximum values of firing shrinkage are attained in specimens fired at 1200 °C for 2 h as shown in Fig. 1(a).

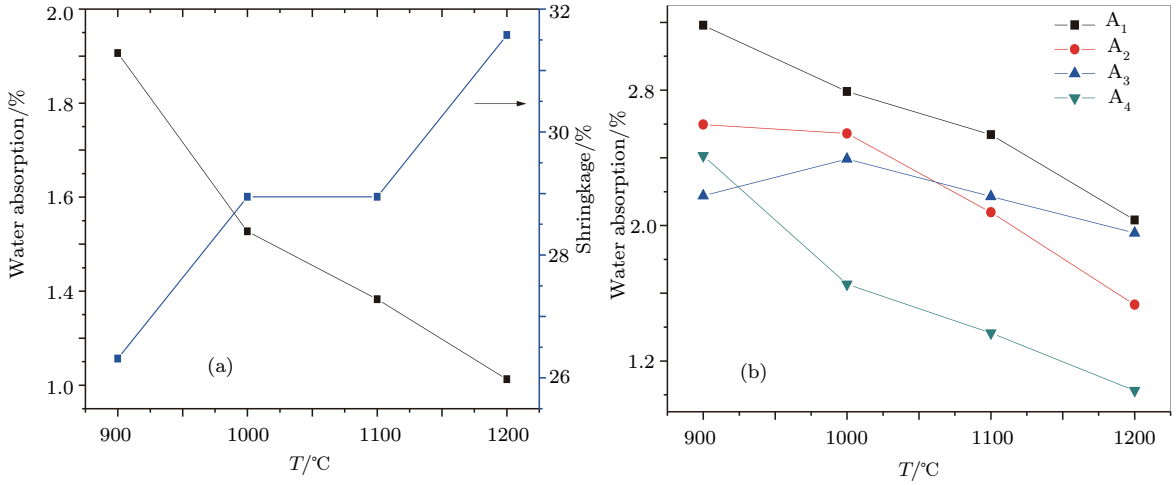


Fig. 1. (color online) (a) Variations of water absorption and shrinkage percentage with sintering temperature of sample A_4 ($x = 0.9$ mol% of TiO_2), and (b) variations of water absorption with sintering temperature of all the prepared samples.

Figure 1(b) shows the relations between the water absorption and the sintering temperature for all the prepared samples. As shown in the figure as sintering temperature increases the water absorption decreases. This is attributed to the increase in the bulk density and the decrease in the porosity.

Higher sintering temperature (above 1200 °C) for 2 h gives rise to the reduction of bulk density. A few pieces of sample A_4 are prepared at different sintering temperatures in a range of 900 °C–1300 °C and the bulk density of the prepared sample is calculated using Archimedes' principle (buoyancy method) and was plotted against the sintering temperature in Fig. 2.

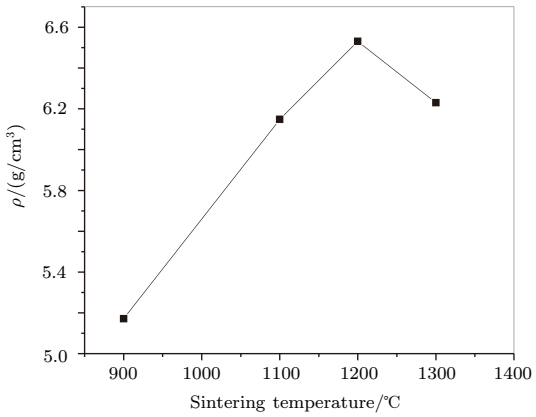


Fig. 2. The bulk density varying with sintering temperature of sample A_4 ($x = 0.9$ mol% of TiO_2).

The results show that the composition exhibits an increase in bulk density at up to 1200 °C after which it starts to decrease. The increase in density is due to increased consolidation with temperature. Densification takes place above 1200 °C. The reduction in bulk density is due to the increase in the amount of porosity between the large grains of ZnO resulting from the rapid grain growth induced by the liquid phase sintering. Similar results were obtained by many authors.[33–35]

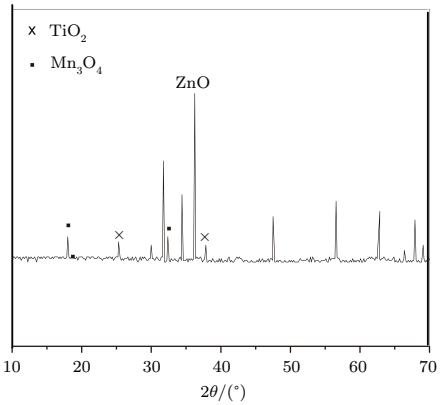


Fig. 3. The XRD patterns of sample (A4) as an example of the prepared samples.

The Bi_2O_3 has a melting point that is far lower than those of ZnO and other additives, and thus exists in liquid phase at a relatively low temperature, which causes other oxides to be distributed evenly in the ZnO grains and grain boundary. The x-ray diffraction (XRD) result of the prepared sample A_4 shows that the main crystal phases are ZnO (JCPDS-36-1451), TiO_2 (JCPDS-84-1286), and Mn_3O_4 can be (JCPDS-01-4837) as shown in Fig. 3. Also the crystal size of ZnO decreases with increasing TiO_2 doping and minimum crystal size appears in sample A_3 as shown in Fig. 4. A similar behavior is observed in ZnO doped with GeO_2 where the average grain size decreases initially as the GeO_2 content increases up to 2 mol%.[36]

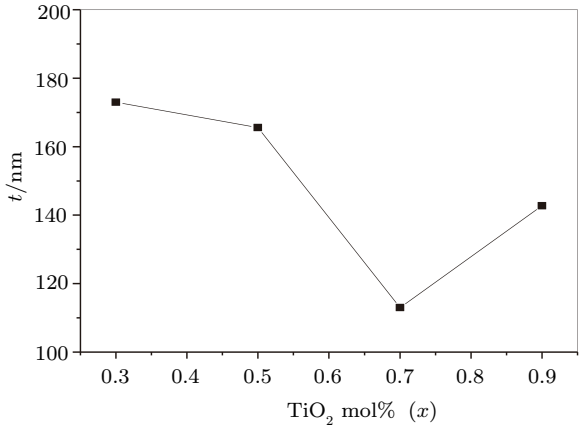


Fig. 4. The variation of the crystallite size with TiO_2 mol% (x).

The decreasing in the crystalline size is attributed to the presence of some TiO_2 and Mn_3O_4 at the grain boundaries which hinder the grain growth and produce an external pressure on the grains and consequently the crystallite size decreases. The microstructure of TiO_2-based ZnO varistor ceramic doped with TiO_2 less than 0.9 mol% mainly consists of two phases: grey bulk phase and white continuous intergranular layer (second phase). The phase composition is further confirmed by EDS. The results reveal that the grey bulk phase is a Zn-rich phase, and the white continuous intergranular layer is a Ti-rich phase as shown in Fig. 5. The SEM of mix A_3 which contains 0.7 mol% of TiO_2 shows two phases, ZnO grains and intergranular phase at triple point, also Ti, Co, and Mn enter into solid solution in the ZnO grain, randomly oriented, Zn is exsoluted accumulating at grain boundaries (white color), grain growth is evident. The EDAX of A_3 shows the distribution of Bi_2O_3, TiO_2, MnO_2, and Co_3O_4 between ZnO–ZnO grains and Ti-rich phase along the grain and intergranular direction. Sung and Kim,[37] and Jing and Zhang[38] reported that, TiO_2 would enhance the reaction activity of the bismuthrich liquid phase and the ZnO phase, and the effect on the ZnO grain growth through the phase boundary reaction. Also it reacts with Bi_2O_3 liquid phase:

$$2Bi_2O_3(l) + 3TiO_2(s) \rightarrow Bi_4(TiO_4)_3.$$

The solubility of ZnO grain in the $Bi_4(TiO_4)_3$ liquid phase is bigger than that in the Bi_2O_3 liquid phase, which will accelerate the speed of ZnO grain transfer in the $Bi_4(TiO4)_3$ liquid phase, and thus will accelerate ZnO grain growth with small grain growth exponent. $Bi_4(TiO_4)_3$ will discompose at a temperature of about 1050 °C and react with ZnO

$$Bi_4(TiO_4)_3(s) + 6ZnO(s) \rightarrow 2Bi_2O_3(l) + 3Zn_2TiO_4.$$

The Zn_2TiO_4 spinel reduces the grain boundary mobility and increases the apparent activation energy.

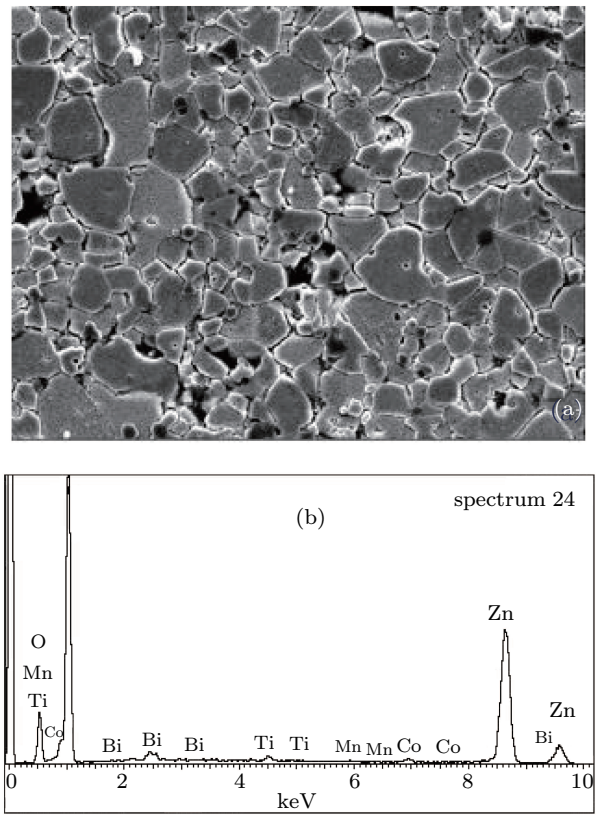


Fig. 5. (a) The SEM image of sample A_3, (b) the EDAX of the above image showing the distribution of Bi_2O_3, TiO_2, MnO_2 with ZnO and Co_3O_4 intergranular accumulation.

The (I–V) characteristics are measured at voltages between 0 kV and 5 kV and currents between 0 mA and 1 mA. The relations between I and V for the different mixes are shown in Fig. 6. It is evident that different mixes show clearly nonlinear behaviors; displaying two regions, i.e., a pre break down in a low voltage region and an off-state and nonlinear properties as an on-state in a high voltage region. The sharper the knee of the curves between the two regions, the better the nonlinearity will be. The nonlinear behavior in ZnO-base material is attributed to the formation of interface state in the band gap of ZnO which leads to the development of potential barriers into electrical conduction at ZnO grain boundaries. Although the intrinsic defects of zinc oxide can account for the formation of such potential barriers in pure ZnO,[39] the presence of external dopants located both at the grain boundaries and inside the grains is expected to change the local configuration, thereby affecting the non-linear behavior of the system. The effect of % TiO_2 on break down voltage is shown in Table 1. Table 1 shows the variations of the nonlinear exponent (α) and the breakdown voltage (V_b) with TiO_2 content. The obtained results of $g\alpha$ show that the nonlinear exponent of the prepared sample increases as TiO_2 molar ratio increases and obtains its maximum value at $x = 0.7$ where a further addition of TiO_2 has a negative effect on the value of α. The increase of α is attributed to the segregation of TiO_2 and Mn_3O_4 on the grain boundaries facilitating the essential potential barrier. So the addition of Tio_2 exhibits an improvement in the non-linear electrical properties of the prepared samples.

Table 1. Calculated values of the nonlinear exponent (α), breakdown voltage ($_{Vb}$) of the prepared samples.

x	α	V_b/kV
0.3	2.993	2
0.5	3.59	3
0.7	8.587	2.5
0.9	0.146	2.8

The results of dielectric constant as a function of frequency at room temperature of different mixes are plotted in Fig. 7. A decrease in capacitance and consequently in dielectric constant is recorded with increasing the frequency ranged (30 kHz–200 kHz). When the applied field is a sinusoidal signal, then the polarization of medium under these AC conditions leads to a dielectric constant that is generally different from the static case. The sinusoidal varying field continuously changes magnitude and direction and it tries to line up the dipoles one-way and then the other way. If the field changes too fast, then the dipoles cannot follow the field and as a consequence remain randomly oriented.[40] Eventually (as shown in Fig. 7) $\varepsilon\prime$ gradually decreases with frequency increasing for all the samples which is known as the dielectric dispersion phenomenon. Similar results were obtained (see Refs. [41], [42], and [43]). The relations between conductivity and frequency for different mixes are shown Fig. 8. This figure indicates that the AC conductivity increases with increasing frequency at room temperature. This may be attributed to the increase in the number of dipoles and consequently increases the hopping probability. Also the increase of frequency raises the conductivity because it increases the ionic response to the field variation. The relations between dielectric constant (ε') and temperature for different samples are shown in Fig. 9. The increase of temperature raises the dielectric constant because it increases ionic response to the field at any particular frequency. These effects are associated with polarization currents arising from trapping states of various kinds.

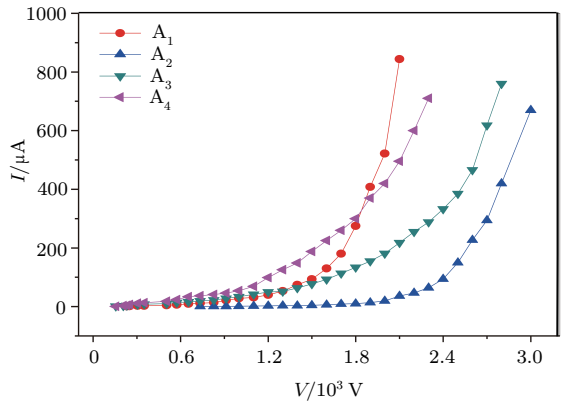


Fig. 6. (color online) The *I*–*V* characteristics of all the prepared samples.

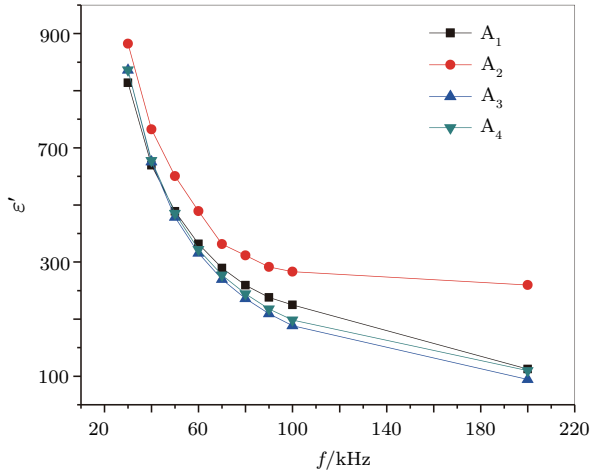


Fig. 7. (color online) The variations of frequency dependence of the dielectric constant of the prepared samples.

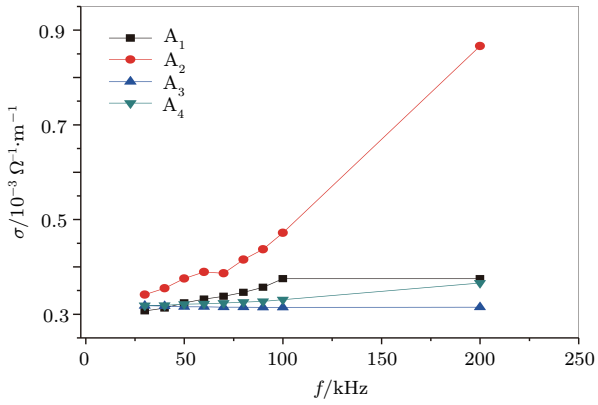


Fig. 8. (color online) The variations of AC conductivity with frequency at room temperature of the prepared samples.

The composition dependences of the dielectric constant and AC conductivity are shown in Fig. 10. This figure exhibits a high dielectric constant and high conductivity at $x = 0.5$. This may be explained in light of the microstructure formed by semi-conductive ZnO grains surrounded by insulating glassy phase which is similar to that of grain boundary layer capacitor. As a result the observed dielectric constant increases with dopant oxide (TiO_2) increasing. In the ZnO–TiO_2 intergranular material interface, the states might be identified with levels in the ZnO or with states lying possibly in the transition region (interface) between ZnO and intergranular material.[44]

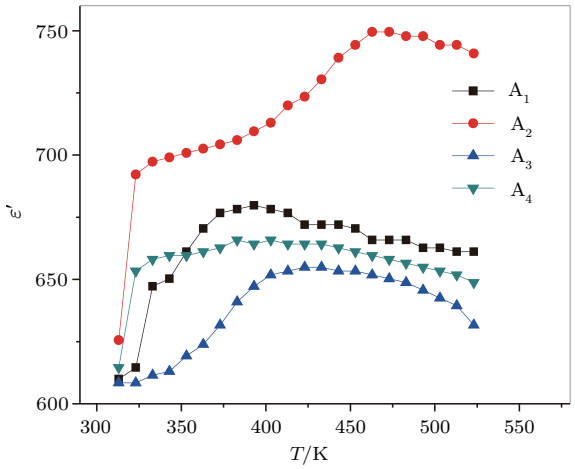


Fig. 9. (color online) The temperature dependences of the dielectric constant of the prepared samples at frequency 30 kHz.

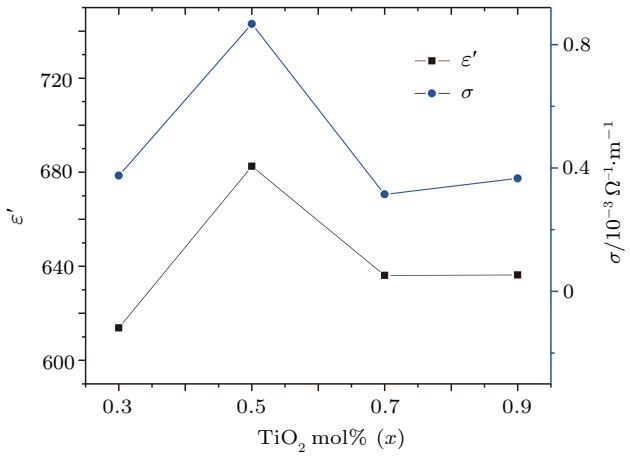


Fig. 10. (color online) The composition dependences of the dielectric constant and AC conductivity at room temperature and 30 kHz.

4. Conclusions

(i) Addition of TiO_2 in the presence of Co_2O_3, MnO_2, and Bi_2O_3 leads to improving densification by minimizing the closed pores. Results of firing shrinkage as a function of temperature show the increase of shrinkage with temperature increasing.

(ii) Maximum values of firing shrinkage and minimum water absorption are attained in specimens fired at 1200 °C for 2 h. So this temperature is selected as the proper temperature for all the samples.

(iii) The Bi_2O_3 is an essential additive of ZnO varistor. It exists in liquid phase at a relatively low temperature, which facilitates other oxide to be distributed evenly in the ZnO grains and grain boundaries.

(iv) The addition of TiO_2 improves the nonlinear coefficient and a further addition above $x = 0.7$ is negatively affected.

(v) A decrease in capacitance and consequently in dielectric constant is recorded with the rise in a frequency range of 30 kHz–200 kHz.

References

[1] Matsuoka M 1971 *Jpn. J. Appl. Phys.* **10** 736
[2] Gupta T K 1990 *J. Am. Ceram. Soc.* **73** 1817
[3] Shichimiya S, Yamaguchi M and Furuse N 1998 *IEEE Trans. Power Deliver.* **13** 465
[4] Clarke D R 1999 *J. Am. Ceram. Soc.* **82** 485
[5] Gupta T K 1990 *J. Am. Ceram. Soc.* **73** 1817
[6] Inada M 1980 *Jpn. J. Appl. Phys.* **19** 409
[7] Olsson E and Dunlop G L 1989 *J. Appl. Phys.* **66** 3666
[8] Tao M, Bui A, Dorlanne O and Loubiere A 1987 *J. Appl. Phys.* **61** 1562
[9] Lee Y S and Tseng T Y 1992 *J. Am. Ceram. Soc.* **75** 1636
[10] Elfwing M, Osterlund R and Olsson E 2001 *J. Am. Ceram. Soc.* **83** 2311
[11] Elfwing M and Olsson E 2000 *J. Am. Ceram. Soc.* **83** 1265
[12] Hng H and Knowles K M 2002 *J. Mater. Sci.* **37** 1143
[13] Han J, Senos A M R and Mantas P Q 2002 *J. Eur. Ceram. Soc.* **22** 1653
[14] Lao Y M, Kuo S T and Tuan W H 2009 *Ceram. Int.* **35** 1317
[15] Einzinger R 1982 *J. Phys. D: Appl. Phys.* **17** 343
[16] Suzuki H and Bradt R C 1995 *J. Am. Ceram. Soc.* **78** 354
[17] Bernik S, Zupancic P and Kolar D 1999 *J. Eur. Ceram. Soc.* **19** 709
[18] Makovec D, Kolar D and Trontelj M 1993 *Mater. Res. Bull.* **28** 803
[19] Bernik S, Daneu N and Recnik A 2004 *J. Eur. Ceram. Soc.* **24** 3703
[20] Wang M H, Yao C and Zhang N F 2008 *J. Mater. Process. Technol.* **202** 406
[21] Mukae K, Tsuda K and Nagasawa I 1977 *Jpn. J. Appl. Phys.* **16** 1361
[22] Alles A B, Puskas R, Callahan G and Burdick V L 1993 *J. Am. Ceram. Soc.* **76** 2098
[23] Lee Y S, Liao K S and Tseng T Y 1996 *J. Am. Ceram. Soc.* **79** 2379
[24] Chun S Y and Mizutani N 2001 *Mater. Sci. Eng. B* **79** 1
[25] Nahm C W and Kim H S 2002 *Mater. Lett.* **56** 379
[26] Nahm C W, Park C H and Yoon H S 2000 *J. Mater. Sci. Lett.* **19** 271
[27] Nahm C W and Park C H 2000 *J. Mater. Sci.* **35** 3037
[28] Nahm C W 2001 *J. Eur. Ceram. Soc.* **21** 545
[29] Nahm C W 2001 *Mater. Lett.* **47** 182
[30] Naham C W and Heo J S 2014 *Trans. Electr. Electr. Mater.* **15** 213
[31] Leach C, Ling Z and Freer R 2001 *J. Eur. Ceram. Soc.* **20** 2759
[32] Baptista J L and Mantas P Q 2000 *J. Electroceram.* **4** 215
[33] Kitouni S and Harabi A 2011 *Ceramica* **57** 453
[34] Badev A, Marinel S, Heuguet R, Savary E and Agrawal D 2013 *Acta Materialia* **61** 7849
[35] Heydari F, Maghsoudipoura A, Shabania MO, Hamnabardb Z and Farhangdousta S 2014 *J. Ceram. Proc. Res.* **15** 35
[36] Desouky O A and Khalil M H 2015 *Int. J. Sci. Res.* **4** 848
[37] Sung G Y and Kim C H 1989 *J. Am. Ceram. Soc.* **22** 61
[38] Fu J and Xu Z. 2003 *J. Electron. Sci. Technol. China* **1** 80
[39] Srikant V, Sergo V and Clarke D R 1995 *J. Am. Ceram. Soc.* **78** 1935
[40] Kasap S O 2002 *Principles Electronic Materials and Devices* (New York: McGraw-Hill) p. 526
[41] Nahm C W 2009 *Trans. Electr. Electron.. Mater.* **10** 80
[42] Yoon J R, Lee C B, Lee K M, Lee H Y and Lee W 2009 *Trans. Electr. Electron. Mater.* **10** 152
[43] Nahm C W 2013 *J. Mater. Sci.: Mater. Electron.* **24** 412
[44] Levinsion L M and Philipp H R 1986 *Am. Ceram. Soc. Bull.* **65** 4639